Wave propagation in a sandwiched layer of transversely isotropic magnetothermoelastic with elastic solids

Parveen Lata [1] , Rajneesh Kumar[2] and Nidhi Sharma[3]
[1]Department of Basic and Applied Sciences, Punjabi University, Patiala, Punjab, India
[2]Department of Mathematics, Kurukshetra University , Kurukshetra, Haryana, India
[3]Department of Mathematics, MM University, Mullana, Ambala, Haryana, India.

Abstract
In the present investigation, a plane P(longitudinal) or SV(transverse) wave is made incident upon a transversely isotropic magnetothermoelastic solid slab of uniform thickness, interposed between two different semi-infinite elastic solids . The transversely isotropic magnetothermoelastic sandwiched layer is homogeneous with combined effects of two temperature, rotation and Hall current in the context of GN Type-II and Type-III (1993)theory of thermoelasticity . The amplitude ratios of various reflected and refracted waves are obtained by using appropriate boundary conditions. The variation of various amplitude ratios with angle of incidence are depicted graphically. Some cases of interest are also deduced from the present investigation.

[1]**Keywords:** Interface**;** Reflection; transmission; transversely isotropic thermoelastic half space ; Amplitude ratios.

1.Introduction

The problem of elastic wave propagation in different media is an important phenomenon in the field of seismology, earthquake engineering and geophysics. The elastic wave propagating through the earth (seismic waves) have to travel through different layers and interfaces. These waves have different velocities and are influenced by the properties of the layer through which they travel. The signals of these waves are not only helpful in providing information about the internal structures of the earth but also helpful in exploration of valuable materials such as minerals, crystals and metals etc. This technique is one of the most suitable in terms of time saving and economy. As the importance of anisotropic devices has increased in many fields of optics and microwaves, wave propagation in anisotropic media has been widely studied over in the last decades. The anisotropic nature basically stems from the polarization or magnetization that can occur in materials when external fields pass by. Mathematical modeling of plane wave propagation along with the free boundary of an elastic half-space has been subject of continued interest for many years (Keith and Crampin (1977) ,Kumar(2015), Kumar and Kansal(2011) ,Marin Marin(2013), Kumar and Mukhopadhyay (2010),Lee and Lee(2010), Kumar and Gupta(2013), Othman(2010), Kaushal, Kumar and Miglani (2011),Kumar , Sharma and Ram(2008)). Chen and Gurtin (1968), Chen et al. (1968) and Chen et al. (1969)have formulated a theory of heat conduction in deformable bodies which depends upon two distinct temperatures, the conductive temperature φ and the thermo dynamical temperature T. For time independent situations, the difference between these two temperatures is proportional to the heat supply, and in absence of heat supply, the two temperatures are identical. For time dependent problems, the two temperatures are different, regardless of the presence of heat supply. The two temperatures T, φ and the strain are found to have representations in the form of a travelling wave plus a response, which occurs

instantaneously throughout the body (Boley and Tolins(1962)).The wave propagation in two temperature theory of thermoelasticity was investigated by Warren and Chen(1973).

Green and Naghdi (1991,1992,1993)postulated a new concept in thermoelasticity theories and proposed three models which are subsequently referred to as GN-I, II, and III models. A comprehensive work has been done in thermoelasticity theory with and without energy dissipation and thermoelasticity with two temperature (Youssef (2011;Youssef (2006);Sharma and Marin(2013); Sharma and Bhargav (2014); Sharma, Kumar,Sharma and Lata(2016)). In view of the fact that most of the large bodies like the earth, the moon and other planets have an angular velocity , as well as earth itself behaves like a huge magnet, it is important to study the propagation of thermoelastic waves in a rotating medium under the influence of magnetic field. So, the attempts are being made to study the propagation of finite thermoelastic waves in an infinite elastic medium rotating with angular velocity. Several authors (Das and Kanoria(2014); Atwa and Jahangir(2014), Hilai and Othman (2016); Ezzat, El-Karamany and El-Bary(2016), Said and Othman (2016), Ailawalia and Singla (2016)) have studied various problems in generalized thermoelasticity to study the various effects. Sandwich structures are widely used in diverse applications such as spacecraft, aircraft, automobiles, boats and ships due to their substantial bending strength and impact resistance at a light weight . The dynamic applications have motivated various studies of wave propagation and dynamic flexural deformation of multilayer beams and plates..Elphinstone and Lakhtakia (1994)have investigated the response of a plane wave incident on a chiral solid slab sandwiched between two elastic half spaces. Khurana and Tomar (2009)discussed longitudinal wave response of chiral slab interposed between micropolar elastic solid half spaces. Wave propagation in sandwich layer has been investigated by many researchers(Chaudhary, Kaushik and Tomar(2010), Deshpande and Fleck(2005), Liu and Bhattacharya(2009),Negin(2016)). Here in this paper, we consider transversely isotropic magnetothermoelastic solid slab of uniform thickness, interposed between two different semi-infinite homogeneous isotropic elastic solids. A plane longitudinal or transverse wave propagating through one of the elastic solid half spaces , is made incident upon transversely isotropic magnetothermoelastic solid. We have presented the reflection and transmission coefficients obtained separately , corresponding to the appropriate set of boundary conditions. The variations in the modulus of the amplitude ratios with the angle of incidence are depicted graphically.

2. Basic Equations

The constitutive relations for a transversely isotropic thermoelastic medium are given by

$$t_{ij} = C_{ijkl}e_{kl} - \beta_{ij}T \qquad (1)$$

Equation of motion for a transversely isotropic thermoelastic medium rotating uniformly with an angular velocity $\boldsymbol{\Omega} = \Omega n$, where n is a unit vector representing the direction of axis of rotation and taking into account Lorentz force

$$t_{ij,j} + F_i = \rho\{\ddot{u}_i + \left(\boldsymbol{\Omega} \times (\boldsymbol{\Omega} \times u)\right)_i + (2\boldsymbol{\Omega} \times \dot{u})_i\} \qquad (2)$$

Following Chandrasekharaia (1998) and Youssef (2006), the heat conduction equation with two temperature and with and without energy dissipation is given by

$$K_{ij}\varphi_{,ij} + K_{ij}^{*}\dot{\varphi}_{,ij} = \beta_{ij}T_0\ddot{e_{ij}} + \rho C_E\ddot{T} \qquad (3)$$

The above equations are supplemented by generalized Ohm's law for media with finite conductivity and including the Hall current effect

$$\boldsymbol{J} = \frac{\sigma_0}{1+m^2}\left(\boldsymbol{E} + \mu_0\left(\dot{\boldsymbol{u}} \times \boldsymbol{H} - \frac{1}{en_e}\boldsymbol{J} \times \boldsymbol{H}_0\right)\right) \quad (4)$$

and the strain displacement relations are

$$e_{ij} = \frac{1}{2}(u_{i,j} + u_{j,i}) \quad i,j = 1,2,3 \quad (5)$$

Here

$F_i = \mu_0(\boldsymbol{J} \times \boldsymbol{H}_0)_i$ are the components of Lorentz force.

$\beta_{ij} = C_{ijkl}\alpha_{ij}$ and $T = \varphi - a_{ij}\varphi_{,ij}$

$\beta_{ij} = \beta_i\delta_{ij}$, $K_{ij} = K_i\delta_{ij}$, $K_{ij}{}^* = K_i{}^*\delta_{ij}$, i is not summed

Following Achenbach(1973),the constitutive relations for the elastic half space are

$$t_{ij,j}{}^l = 2\mu^l u^l_{i,j} + \lambda^l u^l_{k,k}\delta_{ij} \text{ , } (i,j,k = 1,2,3 \ \ and \ l = 1,2) \quad (6)$$

and, equations of motion are

$$\mu^l u^l_{i,jj} + (\lambda^l + \mu^l)u^l_{i,ij} = \rho^e \frac{\partial^2 \boldsymbol{u}_i{}^l}{\partial t^2} \qquad (i,j = 1,2,3 \ \ and \ l = 1,2) \quad (7)$$

$C_{ijkl}(C_{ijkl} = C_{klij} = C_{jikl} = C_{ijlk})$ are elastic parameters, β_{ij} is the thermal tensor, T is the temperature, T_0 is the reference temperature, t_{ij} are the components of stress tensor, e_{kl} are the components of strain tensor,u_i are the displacement components, ρ is the density, C_E is the specific heat, K_{ij} is the thermal conductivity, K^*_{IJ} is the materialistic constant, a_{ij} are the two temperature parameters, α_{ij} is the coefficient of linear thermal expansion, Ω is the angular velocity of the solid, H is the magnetic strength, $\dot{\boldsymbol{u}}$ is the velocity vector , **E** is the intensity vector of the electric field, $\boldsymbol{J}$ **is** the current density vector, $m(= \omega_e t_e = \frac{\sigma_0\mu_0 H_0}{en_e})$ is the Hall parameter, t_e is the electron collision time, $\omega_e = \frac{e\mu_0 H_0}{m_e}$ is the electronic frequency, e is the charge of an electron, m_e is the mass of the electron, $\sigma_0 = \frac{e^2 t_e n_e}{m_e}$, is the electrical conductivity and n_e is the number of density of electrons. λ^l, μ^l , ρ^l are the Lame's constants and density in the elastic half space. $\boldsymbol{u}_i{}^l$ $((i = 1,2,3 \ \ and \ l = 1,2)$ are the components of displacement vector , $t_{ij,j}{}^l$ are the components of stress in elastic half space.

3. Formulation of the problem

Consider a layered model consisting of a transversely isotropic magnetothermoelastic slab of finite thickness H, which is rotating uniformly with an angular velocity **Ω** initially at uniform temperature T_0 with Hall current effect, is interposed between two distinct elastic half spaces. Introducing the Cartesian co-ordinate system (x_1, x_2, x_3) such that x_1 −and x_3 −axis are on horizontal plane and x_3 −axis is pointing vertically downwards. Let the intermediate layer occupying the region $M[0 \le x_3 \le H]$ be delineated by the planes $x_3 = 0$ and $x_3 = H$ as shown in fig1.and the two elastic half spaces be occupying the regions $M^{(1)}: [x_3 < 0]$ and $M^{(2)}: [x_3 > H]$. For two dimensional problem, the displacement vectors $\boldsymbol{u}$, $\boldsymbol{u}^l$ $(l = 1,2)$ in transversely isotropic magnetothermoelastic and in elastic half space are taken as

$\boldsymbol{u} = (u_1, 0, u_3)$ and $\boldsymbol{u}^l = (u^l_1, 0, u^l_3)$, $(l = 1,2)$ (8)

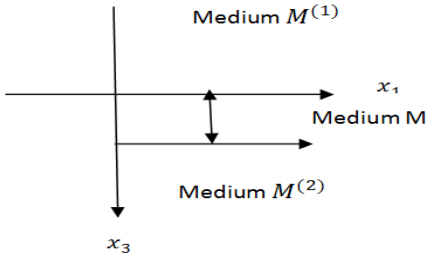

Figure1

We also assume that

$$\boldsymbol{E}=0\,,\quad \boldsymbol{\Omega}=(0,\Omega,0) \tag{9}$$

The generalized Ohm's law gives

$$J_2=0 \tag{10}$$

the current density components J_1 and J_3 using(10) are given as

$$J_1=\frac{\sigma_0\mu_0H_0}{1+m^2}\left(m\frac{\partial u_1}{\partial t}-\frac{\partial u_3}{\partial t}\right) \tag{11}$$

$$J_3=\frac{\sigma_0\mu_0H_0}{1+m^2}\left(\frac{\partial u_1}{\partial t}+m\frac{\partial u_3}{\partial t}\right) \tag{12}$$

Following Slaughter (2002), using appropriate transformations, on the set of equations(2) and (3) and with the aid of (8)-(12), The field equations for transversely isotropic magnetothermoelastic medium are

$$c_{11}\frac{\partial^2u_1}{\partial x^2}+c_{13}\frac{\partial^2u_3}{\partial x_1\partial x_3}+c_{44}\left(\frac{\partial^2u_1}{\partial {x_3}^2}+\frac{\partial^2u_3}{\partial x_1\partial x_3}\right)-\beta_1\frac{\partial}{\partial x_1}\left\{\varphi-\left(a_1\frac{\partial^2\varphi}{\partial {x_1}^2}+a_3\frac{\partial^2\varphi}{\partial {x_3}^2}\right)\right\}-\mu_0J_3H_0=\rho\left(\frac{\partial^2u_1}{\partial t^2}-\Omega^2u_1+2\Omega\frac{\partial u_3}{\partial t}\right) \tag{13}$$

$$(c_{13}+c_{44})\frac{\partial^2u_1}{\partial x_1\partial x_3}+c_{44}\frac{\partial^2u_3}{\partial {x_1}^2}+c_{33}\frac{\partial^2u_3}{\partial {x_3}^2}-\beta_3\frac{\partial}{\partial x_3}\left\{\varphi-\left(a_1\frac{\partial^2\varphi}{\partial {x_1}^2}+a_3\frac{\partial^2\varphi}{\partial {x_3}^2}\right)\right\}+\mu_0J_1H_0=\rho\left(\frac{\partial^2u_3}{\partial t^2}-\Omega^2u_3-2\Omega\frac{\partial u_1}{\partial t}\right) \tag{14}$$

$$\left(k_1+{k_1}^*\frac{\partial}{\partial t}\right)\frac{\partial^2\varphi}{\partial {x_1}^2}+\left(k_3+{k_3}^*\frac{\partial}{\partial t}\right)\frac{\partial^2\varphi}{\partial {x_3}^2}=T_0\frac{\partial^2}{\partial t^2}\left\{\beta_1\frac{\partial u_1}{\partial x_1}+\beta_3\frac{\partial u_3}{\partial x_3}\right\}+\rho C_E\ddot{T} \tag{15}$$

and the stress components are

$$t_{33}=c_{13}e_{11}+c_{33}e_{33}-\beta_3T \tag{16}$$

$$t_{13}=2c_{44}e_{13} \tag{17}$$

where

$$T=\varphi-\left(a_1\frac{\partial^2\varphi}{\partial x_1^2}+a_3\frac{\partial^2\varphi}{\partial x_3^2}\right)$$

$$\beta_1=(c_{11}+c_{12})\alpha_1+c_{13}\alpha_3\,,\qquad \beta_3=2c_{13}\alpha_1+c_{33}\alpha_3$$

In the above equations we use the contracting subscript notations $(11\rightarrow 1, 22\rightarrow 2, 33\rightarrow 3, 23\rightarrow 4, 31\rightarrow 5, 12\rightarrow 6)$ to relate $c_{ijkl}\ to\ c_{mn}$

The field equations for the elastic half spaces are

$$\mu^l\left(\frac{\partial^2u_1^l}{\partial {x_1}^2}+\frac{\partial^2u_1^l}{\partial {x_3}^2}\right)+\left(\lambda^l+\mu^l\right)\frac{\partial^2u_3^l}{\partial x_1\partial x_3}=\rho^l\frac{\partial^2{u_1}^l}{\partial t^2}\quad,\quad (l=1,2) \tag{18}$$

$$\mu^l\left(\frac{\partial^2u_3^l}{\partial {x_1}^2}+\frac{\partial^2u_3^l}{\partial {x_3}^2}\right)+\left(\lambda^l+\mu^l\right)\frac{\partial^2u_1^l}{\partial x_1\partial x_3}=\rho^l\frac{\partial^2{u_3}^l}{\partial t^2}\qquad (l=1,2) \tag{19}$$

The stress components for elastic half spaces in the x_1-x_3 plane are

$$t_{13}^l=\mu^l\left(\frac{\partial {u_1}^l}{\partial x_3}+\frac{\partial {u_3}^l}{\partial x_1}\right)\ ,(l=1,2) \tag{20}$$

$$t_{33}^{l} = (\lambda^{l})\frac{\partial {u_1}^{l}}{\partial x_1} + (\lambda^{l} + 2\mu^{l})\frac{\partial {u_3}^{l}}{\partial x_3} \quad , (l = 1,2) \qquad (21)$$

To facilitate the solution, we introduce the dimensionless quantities

$$x_1' = \frac{x_1}{L}\ ,\ x_3' = \frac{x_3}{L}\ ,\ (u_1', u_3', {u_1}'^{l}, {u_3}'^{l}) = \frac{\rho c_1^2}{L\beta_1 T_0}(u_1, u_3, {u_1}^{l}, {u_3}^{l})\ , T' = \frac{T}{T_0}\ , t' = \frac{c_1}{L}t\ , t_{11}' = \frac{t_{11}}{\beta_1 T_0},$$

$$J' = \frac{\rho c_1^2}{\beta_1 T_0} J(t_{33}', t_{31}', t_{13}'^{l}, t_{33}'^{l}) = (\frac{t_{33}}{\beta_1 T_0}, \frac{t_{31}}{\beta_1 T_0}, \frac{t_{13}^{l}}{\beta_1 T_0}, \frac{t_{33}^{l}}{\beta_1 T_0})\ ,\ \varphi' = \frac{\varphi}{T_0}\ , a_1' = \frac{a_1}{L}\ , a_3' = \frac{a_3}{L}\ ,\ h' = \frac{h}{H_0}$$

$$M = \frac{\sigma_0 \mu_0 H_0}{\rho c_1 L}\ , \Omega' = \frac{L}{c_1}\Omega \quad \text{where} \quad c_{11} = \rho c_1^2 \qquad (22)$$

Using dimensionless quantities defined by (22) in the equations (13)-(15) and (18)-(19), and suppressing the primes, the resulting equations yield

$$\frac{\partial^2 u_1}{\partial {x_1}^2} + \delta_4 \frac{\partial^2 u_3}{\partial x_1 \partial x_3} + \delta_2 \left(\frac{\partial^2 u_1}{\partial {x_3}^2} + \frac{\partial^2 u_3}{\partial x_1 \partial x_3}\right) - \frac{\partial}{\partial x_1}\left\{\varphi - \left(\frac{a_1}{L}\frac{\partial^2 \varphi}{\partial {x_1}^2} + \frac{a_3}{L}\frac{\partial^2 \varphi}{\partial {x_3}^2}\right)\right\} - \frac{M}{1+m^2}\mu_0 H_0 \left(\frac{\partial u_1}{\partial t} + m\frac{\partial u_3}{\partial t}\right) = \frac{\partial^2 u_1}{\partial t^2} - \Omega^2 u_1 + 2\Omega \frac{\partial u_3}{\partial t} \qquad (23)$$

$$\delta_1 \frac{\partial^2 u_1}{\partial x_1 \partial x_3} + \delta_2 \frac{\partial^2 u_3}{\partial {x_1}^2} + \delta_3 \frac{\partial^2 u_3}{\partial {x_3}^2} - \frac{\beta_3}{\beta_1}\frac{\partial}{\partial x_3}\left\{\varphi - \left(\frac{a_1}{L}\frac{\partial^2 \varphi}{\partial {x_1}^2} + \frac{a_3}{L}\frac{\partial^2 \varphi}{\partial {x_3}^2}\right)\right\} + \frac{M}{1+m^2}\mu_0 H_0 \left(m\frac{\partial u_1}{\partial t} - \frac{\partial u_3}{\partial t}\right) = \frac{\partial^2 u_3}{\partial t^2} - \Omega^2 u_3 - 2\Omega \frac{\partial u_1}{\partial t} \qquad (24)$$

$$\varepsilon_1 \left(1 + \frac{\varepsilon_3}{\varepsilon_1}\frac{\partial}{\partial t}\right)\frac{\partial^2 \varphi}{\partial {x_1}^2} + \varepsilon_2 \left(1 + \frac{\varepsilon_4}{\varepsilon_2}\frac{\partial}{\partial t}\right)\frac{\partial^2 \varphi}{\partial {x_3}^2} = {\varepsilon_5}'{\beta_1}^2 \frac{\partial^2}{\partial t^2}\left(\frac{\partial u_1}{\partial x_1} + \frac{\beta_3}{\beta_1}\frac{\partial u_3}{\partial x_3}\right) + \frac{\partial^2}{\partial t^2}\left(\left\{\varphi - \frac{a_1}{L}\frac{\partial^2 \varphi}{\partial {x_1}^2} + \frac{a_3}{L}\frac{\partial^2 \varphi}{\partial {x_3}^2}\right\}\right) \qquad (25)$$

$$\delta_1 = \frac{(c_{13}+c_{44})}{c_{11}}\ , \delta_2 = \frac{c_{44}}{c_{11}}\ , \delta_3 = \frac{c_{33}}{c_{11}}\ , \delta_4 = \frac{c_{13}}{c_{11}}\ ,\quad \varepsilon_1 = \frac{k_1}{\rho C_E c_1^2}\ , \varepsilon_2 = \frac{k_3}{\rho C_E c_1^2}\ ,\ \varepsilon_3 = \frac{{k_1}^*}{L\rho C_E c_1}$$

$$\varepsilon_4 = \frac{{k_3}^*}{L\rho C_E c_1} \qquad {\varepsilon_5}' = \frac{T_0}{\rho^2 C_E c_1^2}$$

For the mediums $M^{(1)}$ and $M^{(2)}$, we have

$$\nabla^2 \phi^l = \frac{1}{(\alpha'^{(l)})^2}\left(\frac{\partial^2 \varphi^l}{\partial t^2}\right) \qquad (26)$$

$$\nabla^2 \psi^l = \frac{1}{\beta'^{(l)^2}}\left(\frac{\partial^2 \psi^l}{\partial t^2}\right) \qquad (27)$$

where

$\alpha'^{(l)} = \frac{\alpha^{(l)}}{c_1}$, $\beta'^{(l)} = \frac{\beta^{(l)}}{c_1}$, $\alpha^{(l)} = \sqrt{\frac{(\lambda^l + 2\mu^l)}{\rho^l}}$ and $\beta^{(l)} = \sqrt{\frac{\mu^l}{\rho^l}}$ are velocities of longitudinal and transverse waves respectively for the mediums $M^{(1)}$ and $M^{(2)}$ for $(l = 1,2)$ and ϕ^l and ψ^l are the scalar potentials defined by

$$u_1^l = \frac{\partial \phi^l}{\partial x_1} - \frac{\partial \psi^l}{\partial x_3}, \quad u_3^l = \frac{\partial \phi^l}{\partial x_3} + \frac{\partial \psi^l}{\partial x_1} \qquad (28)$$

We seek a wave solution of the form for transversely isotropic magnetothermoelastic solid as

$$\begin{pmatrix} u_1 \\ u_3 \\ \varphi \end{pmatrix} = \begin{pmatrix} U_1 \\ U_3 \\ \varphi^* \end{pmatrix} \exp\{(ik(x_1 sin\theta + x_3 cos\theta) - i\omega t)\} \qquad (29)$$

where $(sin\theta, cos\theta)$ denotes the projection of the wave normal onto the $x_1 - x_3$ plane, k and ω are respectively the wave number and angular frequency of plane waves propagating in $x_1 - x_3$ plane. Upon using (29) in (23)-(25) and then eliminating $U_1, U_3\ and\ \varphi^*$ from the resulting equations yields the following characteristic equation

$$Ak^6 + Bk^4 + Ck^2 + D = 0 \qquad (30)$$

where , *B* , *C, D* are given in appendix A.

The roots of equation (30) gives six values of , in which we are interested to those roots whose imaginary parts are positive. Corresponding to these roots, there exists three waves corresponding to decreasing orders of their velocities, namely quasi-longitudinal , quasi-transverse and quasi-thermal waves . The phase velocity is given by

$$V_j = \frac{\omega}{|Re(k_j)|}, \quad j=1,2,3$$

where V_j, j=1,2,3 are the phase velocities of QL, QTS and QT waves respectively.

4.Wave Solution

Let a plane P or SV wave travelling through the elastic half space $M^{(1)}$ be incident at the interface $x_3 = 0$ and makes an angle $\theta_0^{(1)}$ with the x_3 −axis.A part of this incident energy will be reflected back into the medium $M^{(1)}$ and rest will be transmitted into the medium M. Now the wave associated with transmitted energy will proceed through the medium M to interact with the boundary $x_3 = H$, where again some part of this energy will be reflected and rest will be transmitted into the medium $M^{(2)}$. The reflected energy further proceeds back to interact with the boundary $x_3 = 0$, and the process will repeat. To satisfy the boundary conditions at both the interfaces ,i.e. $x_3 = 0$ and $x_3 = H$, we shall take the following reflected and refracted waves into consideration.

A plane longitudinal or transverse wave , making an angle θ_0 with the x_3 −axis is incident at the interface through the elastic half space $M^{(1)}$. This wave results in

Reflected waves

(i). One reflected longitudinal wave travelling with speed $\alpha^{(1)}$ and making an angle $\theta_1^{(1)}$ with the x_3 −axis and one transverse wave propagating with speed $\beta^{(1)}$ and making an angle $\theta_2^{(1)}$ with the x_3 −axis in the medium $M^{(1)}$.

(ii) A reflected longitudinal wave, transverse wave and a thermal wave travelling with speeds v_1 , v_2 and v_3 and making angles θ_1, θ_2 and θ_3 with x_3 −axis in the medium *M*.

Refracted waves

(i) A set consisting of longitudinal wave, transverse wave and a thermal wave travelling with speeds v_1 , v_2 and v_3 and making angles θ_1, θ_2 and θ_3 with x_3 −axis In the medium M.

(ii) A longitudinal wave travelling with speed $\alpha^{(2)}$ and making an angle $\theta_1^{(2)}$ with the x_3 −axis and one transverse wave propagating with speed $\beta^{(2)}$ and making an angle $\theta_2^{(2)}$ with the x_3 −axis in the medium $M^{(2)}$.

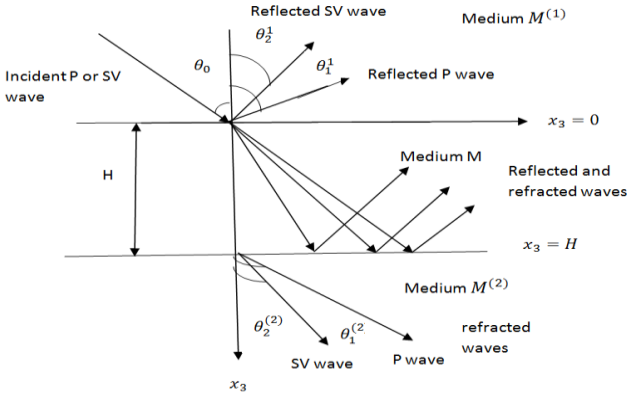

Fig2. Geometry of the problem

We assume the wave solution for the mediums *M*, $M^{(1)}$ and $M^{(2)}$ as

Medium M: $u_1 = \sum_{j=1}^{3}(A_j P_j^{+}) + \sum_{j=4}^{6}(A_j P_{j-3}^{-})$ (31)

$u_3 = \sum_{j=1}^{3}(d_j A_j P_j^{+}) + \sum_{j=4}^{6}(d_j A_j P_{j-3}^{-})$ (32)

$\varphi = \sum_{j=1}^{3}(l_j A_j P_j^{+}) + \sum_{j=4}^{6}(l_j A_j P_{j-3}^{-})$ (33)

where the coupling constants d_j and l_j are given in Appendix B.

Medium $M^{(1)}$: $\phi^{(1)} = A_0^{(1)} P_0^{+(1)} + A_1^{(1)} P_0^{-(1)}$ (34)

$\psi^1 = B_0^{(1)} Q_1^{+(1)} + B_1^{(1)} Q_1^{-(1)}$ (35)

Medium $M^{(2)}$: $\phi^{(2)} = A_0^{(2)} P_0^{+(2)}$, (36)

$\psi^{(2)} = B_0^{(2)} Q_1^{+(2)}$ (37)

Where $P_0^{+(l)} = \exp[i\omega\{(\sin\theta_0^{(l)} x_1 + cos\theta_0^{(l)} x_3)/\alpha'^{(l)} - t\}]$, $l = 1,2$

$P_0^{-(1)} = \exp[i\omega\{$

$Q_1^{+(i)} = \exp[i\omega\{$

$Q_1^{-(1)} = \exp[i\omega\{$

$P_j^{+} = \exp\{ik_j(\sin\theta_j x_1 + cos\theta_j x_3) - i\omega t\}$

$P_j^{-} = \exp\{ik_j(\sin\theta_j x_1 - cos\theta_j x_3) - i\omega t\}$,j=1,2,3 where $k_j = \omega/v_j$

5.Boundary conditions

B.(1)The boundary conditions to be satisfied at the interface $x_3 = 0$ are:

(i) continuity of the stress component $t_{33} = t_{33}^{(1)}$ (38)

(ii) $t_{31} = t_{31}^{(1)}$ (39)

(iii) Continuity of displacement components $u_1 = u_1^{(1)}$ (40)

(iv) $u_3 = u_3^{(1)}$ (41)

(v) Thermally insulated boundary $\frac{\partial\varphi}{\partial x_3} = 0$ (42)

B.(2) The boundary conditions to be satisfied at the interface $x_3 = H$ are:

(i) continuity of the stress component $t_{33} = t_{33}^{(2)}$ (43)

(ii) $t_{31} = t_{31}^{(2)}$ (44)

(iii) Continuity of displacement components $u_1 = u_1^{(2)}$ (45)

(iv) $u_3 = u_3^{(2)}$ (46)

(v) Thermally insulated boundary $\frac{\partial \varphi}{\partial x_3} = 0$ (47)

Amplitude Ratios

Incident P wave

Using equations (31)-(37) in the equations (38)-(47) with the aid of (23)-(27) , we obtain a non homogeneous system of equations

AX=B (48)

where A=$\left[a_{ij}\right]_{10\times 10}$, $X = [z_1, z_2, z_3, z_4, z_5, z_6, z_7, z_8, z_9, z_{10}]^t$, where 't' in the superscript represents the transpose of the matrix, $z_1 = \frac{A_1^{(1)}}{A_0^{(1)}}$, $z_2 = \frac{B_1^{(1)}}{A_0^{(1)}}$ are the reflection coefficients in the medium $M^{(1)}$, $z_i = \frac{A_i}{A_0^{(1)}}, i = 3,4,5$ are the transmission coefficients in the medium M ,$z_i = \frac{A_i}{A_0^{(1)}}$, $i = 6,7,8$ are the reflection coefficients in the medium M, $z_9 = \frac{A_0^{(2)}}{A_0^{(1)}}, z_{10} = \frac{B_0^{(2)}}{A_0^{(1)}}$ are the reflection coefficients in the medium $M^{(2)}$. Using Cramer's rule, the system of equations given in (48) enables us to amplitude ratios of various reflected and transmitted waves. The values of a_{ij} and B are given in appendix C.

Incident SV wave

In system of equations (48), if we replace $A_0^{(1)}$ by $B_0^{(1)}$ and equate $A_0^{(1)} = 0$, we obtain the amplitude ratios corresponding to incident SV wave.

6.Particular cases

(i) If $k_1^* = k_3^* = 0$, then from appendix C ,we obtain the corresponding expressions for transversely isotropic magnetothermoelastic solid slab of uniform thickness , interposed between two different semi-infinite elastic solids without energy dissipation and with two temperature with Hall current effect and rotation.

(ii) If $a_1 = a_3 = 0$, then we obtain the expressions for transversely isotropic magnetothermoelastic solid slab of uniform thickness , interposed between two different semi-infinite elastic solids with and without energy dissipation alongwith with Hall current effect and rotation.

(iii) If we take $c_{11} = \lambda + 2\mu = c_{33}$, $c_{12} = c_{13} = \lambda$, $c_{44} = \mu, \beta_1 = \beta_3 = \beta, \alpha_1 = \alpha_3 = \alpha, K_1 = K_3 = K$ and $a_1 = a_3 = a$, we obtain the corresponding expressions in isotropic magnetothermoelastic solid slab of uniform thickness , interposed between two different semi-infinite elastic solids with two temperature and with and without energy dissipation alongwith combined effects of Hall current and rotation.

7.Numerical results and discussion

For the purpose of numerical evaluation,

i) Cobalt material has been chosen for transversely isotropic magnetothermoelastic solid (medium M), following Dhaliwal and Singh(1980), as $c_{11} = 3.071 \times 10^{11} Nm^{-2}, c_{12} = 1.650 \times 10^{11} Nm^{-2}, c_{33} = 3.581 \times 10^{11} Nm^{-2}$, $c_{13} = 1.027 \times 10^{11} Nm^{-2}$, $c_{44} = 1.510 \times 10^{11} Nm^{-2}$,$\rho = 8.836 \times 10^3 Kgm^{-3}$, $T_0 = 298°K, C_E = 4.27 \times 10^2 JKg^{-1}deg^{-1}$, $K_1 = .690 \times 10^2 wm^{-1}deg^{-1}$, , $K_3 = .690 \times 10^2 wm^{-1}deg^{-1}$, $\beta_1 = 7.04 \times 10^6 Nm^{-2}deg^{-1}$, $\beta_3 = 6.90 \times 10^6 Nm^{-2}deg^{-1}, K_1^* = 0.02 \times$

$10^2 Nsec^{-2}deg^{-1}$, $K_3^* = 0.04 \times 10^2 Nsec^{-2}deg^{-1}$, $\mu_0 = 1.2571 \times 10^{-6} Hm^{-1}$, $H_0 = 1 Jm^{-1}nb^{-1}$,$\varepsilon_0 = 8.838 \times 10^{-12} Fm^{-1}$ with non-dimensional parameter L=1 and $\sigma_0 = 9.36 \times 10^5 col^2/Cal.cm.$sec, Ω=3, $t_0 = 0.02$, M=3 and two temperature parameters is taken as a_1=0.03 and a_3=0.06.

ii) Copper material has been chosen for elastic solid (medium M(1)), following Youssef(2006) as

$\lambda = 7.76 \times 10^{10}\ Kgm^{-1}s^{-2}$, $\mu = 3.278 \times 10^{10}\ Kgm^{-1}s^{-2}$, $C_E = 0.6331 \times 10^3 JKg^{-1}K^{-1}$ $\rho = 8.954 \times 10^3 Kgm^{-3}$. .

iii)Following Dhaliwal and Singh(1980), Magnesium material has been taken for the medium M(2) as

$\lambda = 2.17 \times 10^{10} Nm^2$, $\mu = 3.278 \times 10^{10} Nm^2$,$\omega_1 = 3.58 \times 10^{11} S^{-1}$, $\rho = 1.74 \times 10^3 Kgm^{-3}$, $T_0 = 298$K , $C_E = 1.04 \times 10^3 Jkg^{-1}deg^{-1}$

Matlab software 8.4.0. has been used for numerical computation of the resulting quantities. The values of Amplitude ratios of various reflected and refracted waves, when P wave or SV wave is incident , with respect to angle of incidence θ have been computed and are depicted graphically in figures3-23. A comparison has been made to show the magnetic effect and the two theories of GN Type-II and GN Type-III . In the figures 3-22

1). Solid line corresponds to GN theory of Type-III
2). The small dashed line with centre symbol circle corresponds to GN theory of Type-II.
3) The long dashed line with centre symbol cross corresponds to Hall parameter m=0.

Incident P Wave

Amplitude ratio $\mathbf{Z_1}$: Fig.3 exhibits the variations of amplitude ratio Z_1 with angle of incidence θ . We notice that the variations increase sharply corresponding to M=0, for the range $0^0 \leq \theta \leq 20^0$. When θ approaches 20^0, we notice a sharp decrease approaching the boundary surface and remain stationary for the rest. For GN Theory of Type -II and Type-III variations are similar (as for M=0) for the range $0^0 \leq \theta \leq 40^0$ and when θ moves further, a small jump is noticed in the range $40^0 \leq \theta \leq 45^0$ followed by small variations in the rest for GN theory of Type-II, whereas for GN theory of Type-III, the values of amplitude ratio are constant for the range $20^0 \leq \theta \leq 75^0$, followed by a small fall for the range $75^0 \leq \theta \leq 85^0$ and small variations are noticed afterwards.

Amplitude ratio $\mathbf{Z_2}$: Fig.4 exhibits the variations of amplitude ratio Z_2 with angle of incidence θ. Here, we notice that corresponding to all the cases , variations are similar with a sharp jump in the values of amplitude ratio for the range $0^0 \leq \theta \leq 20^0$ and are negligible afterwards. Maximum values are noticed corresponding to GN theory of Type-II.

Amplitude ratio $\mathbf{Z_3}$: Fig.5 shows the trends of variations of amplitude ratio Z_3 with angle of incidence θ. Here, we notice that corresponding to GN theory of Type-III, the variations are in form of seismic waves for the whole range with less magnitude for the range $0^0 \leq \theta \leq 60^0$ and achieving maximum magnitude for $60^0 \leq \theta \leq 70^0$. For GN theory of Type -II, a sharp increase in the values of amplitude ratio with maximum magnitude is noticed for the range $10^0 \leq \theta \leq 30^0$, and stationary trend is noticed in the rest. Corresponding to M=0, trends of variations are similar to GN theory of Type-II with less magnitude.

Amplitude ratio $\mathbf{Z_4}$: Fig.6 exhibits the trends of variations of amplitude ratio Z_4 with angle of incidence θ. We notice that for GN Type-II, initially the values of Z_4 lie on the boundary surface but as θ approaches 20^0, a sudden jump in the variations is noticed similar to Dirac delta function and when θ moves away i.e. farther from 40^0, variations with small magnitudes are noticed above the boundary surface. For GN theory of Type-III, variations are in form of seismic wave when θ moves away from 30^0 as prior to this range the values lie on the boundary surface. For M=0, small variations near boundary surface are noticed for the whole range except for $10^0 \leq \theta \leq 20^0$ as here the variations are instant and achieve maximum values.

Amplitude ratio $\mathbf{Z_5}$: Fig.7 shows the trends of variations of amplitude ratio Z_5 with angle of incidence θ. We notice that initially the values are steady state for all the cases but as θ approaches 20^0, the values of amplitude ratio start varying. For GN Type-II and Type-III, the values are in form of seismic waves with different patterns. Value corresponding to GN Type-II reach to the maximum at $\theta = 60^0$ whereas corresponding to GN Type-III, maximum values are achieved for $\theta > 90^0$. However variations in form of oscillations above boundary surface are noticed corresponding to M=0.

Amplitude ratio $\mathbf{Z_6}$: Fig.8 displays the variations of amplitude ratio Z_6 with angle of incidence θ. Here corresponding to GN theory of Type-III, the values of amplitude ratio move away from the boundary surface in form of ascending pattern of waves as θ increases whereas the trends are different corresponding to GN Type -II, as here the variations approach boundary surface away from the initial range with small variations. For the initial range, a sharp increase followed by sharp decrease is noticed. For M=0, for the range $5^0 \leq \theta \leq 15^0$, the values are in form of Dirac delta function with less amplitude and the pattern is oscillatory near the boundary surface in the rest.

Amplitude ratio $\mathbf{Z_7}$: Fig.9 displays the variations of amplitude ratio Z_7 with angle of incidence θ. It is noticed that corresponding to GN Type-II, the variations are in form of Dirac delta function for the range $10^0 \leq \theta \leq 30^0$ and remain negligible for the rest. For M=0, similar variations are noticed with difference of range as to GN-II. Corresponding to GN Type-III, the variations increase as θ increases and follow the pattern of ascending seismic waves moving away from the boundary surface .

Amplitude ratio $\mathbf{Z_8}$: Fig.10 displays the variations of amplitude ratio Z_8 with angle of incidence θ. It is evident that corresponding to GN Type-II and for M=0, trends with sharp increase and sharp decrease are noticed for the whole range whereas maximum variations are noticed corresponding to GN Type-III, for the second half range and reaching to maximum at the end and remain near the boundary surface for the first half range.

Amplitude ratio $\mathbf{Z_9}$: Fig.11 exhibits the variations of amplitude ratio Z_9 with angle of incidence θ. It is evident that corresponding to GN Type-II, initially, a sharp decrease is seen and oscillatory pattern is noticed afterwards. Corresponding to GN Type-III, the variations are in form of Dirac delta function for the range $5^0 \leq \theta \leq 15^0$ and are negligible for the rest. For M=0, the variations are similar to GN theory of Type-III with small magnitude.

Amplitude ratio $\mathbf{Z_{10}}$: Fig12. displays the variations of amplitude ratio Z_{10} with angle of incidence θ. Corresponding to all the cases, initially the value of amplitude ratio are very high followed by a sharp decrease and small in the rest.

Incident SV Wave

Amplitude ratio $\mathbf{Z_1}$: Fig.13, exhibits the variations of amplitude ratio Z_1 with angle of incidence θ. Here, we notice that the trends of variations are similar corresponding to the three cases upto $\theta = 40^0$, as θ crosses 40^0, then corresponding to M=0, variations are in form of Dirac Delta function for the range $40^0 \leq \theta \leq 50^0$ and after this range descending oscillatory behaviour is noticed. Corresponding to GN-II, for the range $40^0 \leq \theta \leq 60^0$, the trends are descending oscillatory and as θ approaches 60^0, a sharp increase followed by a sharp decrease is noticed and again the behaviour is descending oscillatory. Corresponding to GN-III, a smooth decrease is noticed for the rest of the range.

Amplitude ratio $\mathbf{Z_2}$: Fig.14 exhibits the variations of amplitude ratio Z_2 with angle of incidence θ, when SV Wave is incident. Here, we notice that corresponding to all the cases , variations are similar with a sharp jump in the values of amplitude ratio for the range $20^0 \leq \theta \leq 40^0$ and the variations differ for the rest of the range corresponding to three cases. Corresponding to GN-III, smooth increase is noticed for the range $\theta \geq 40^0$ .Corresponding to GN-II, ascending oscillatory trends are noticed. whereas corresponding to M=0, a sharp jump is noticed at $\theta = 60^0$ followed by small variations afterwards.

Amplitude ratio $\mathbf{Z_3}$:Fig.15 shows the trends of variations of amplitude ratio Z_3 with angle of incidence θ. Here, we notice that corresponding to GN Type-III and GN Type-II, the variations are in form of seismic waves for the whole range with less magnitude for the range $0^0 \leq \theta \leq 40^0$. Corresponding to M=0, initially the trends are same and a sharp increase in the values of amplitude ratio with maximum magnitude is noticed at $\theta = 50^0$, and stationary trend is noticed in the rest.

Amplitude ratio $\mathbf{Z_4}$: Fig.16 exhibits the trends of variations of amplitude ratio Z_4 with angle of incidence θ. We notice that for GN Type-II, initially the values of Z_4 lie on the boundary surface but as θ approaches 40^0, a sudden jump in the variations is noticed similar to Dirac delta function and when θ moves away i.e. farther from 50^0, same trends are repeated. For GN theory of Type-II, variations repeat in the form of Dirac Delta function for the range $50^0 \leq \theta \leq 70^0$ and small variations are noticed afterwards.

Amplitude ratio $\mathbf{Z_5}$: Fig.17 shows the trends of variations of amplitude ratio Z_5 with angle of incidence θ. We notice that initially the values are steady state for all the cases but as θ approaches 20^0, the values of amplitude ratio start varying. For GN Type-III, the values are in form of seismic waves .Value corresponding to GN Type-II reach to the maximum at $\theta = 60^0$ whereas corresponding to M=0,maximum values are achieved for $\theta = 50^0$.

Amplitude ratio $\mathbf{Z_6}$: Fig.18 displays the variations of amplitude ratio Z_6 with angle of incidence θ. Here corresponding to GN theory of Type-III, the values of amplitude ratio move away from the boundary surface in form of ascending pattern of waves as θ increases whereas the trends are different corresponding to GN Type -II, as here the variations approach boundary surface away from the initial range with small variations. For the initial range, a sharp increase followed by sharp decrease is noticed.

For M=0, for the range $5^0 \leq \theta \leq 15^0$, the values are in form of Dirac delta function with less amplitude and the pattern is oscillatory near the boundary surface in the rest.

Amplitude ratio Z_7: Fig.19 displays the variations of amplitude ratio Z_7 with angle of incidence θ. It is noticed that corresponding to GN Type-III, the variations are in form of seismic waves. Corresponding to M=0 and GN Type-II, trends are similar with change in magnitudes with maximum variations for the range $45^0 \leq \theta \leq 65^0$.

Amplitude ratio Z_8: Fig.20 displays the variations of amplitude ratio Z_8 with angle of incidence θ. Here similar trends are noticed as in figure 20 with change in magnitude.

Amplitude ratio Z_9: Fig.21 exhibits the variations of amplitude ratio Z_9 with angle of incidence θ. Corresponding to GN Type-II, initially, a sharp decrease is seen and the values of amplitude ratio remain stationary for the range $20^0 \leq \theta \leq 30^0$,and as θ approaches 30^0 , increase in form of step is noticed up to $\theta = 35^0$ and the values remain stationary upto $\theta = 60^0$, a decrease is seen at $\theta = 60^0$ followed by a sharp jump for the range $60^0 \leq \theta \leq 70^0$ and a small jump for the range $70^0 \leq \theta \leq 75^0$. As θ crosses 75^0, a loop in the downwards direction is noticed , then remaining stationary goes down at $\theta = 95^0$. Corresponding to GN Type-III, the variations are in form of Dirac Delta function for the range $10^0 \leq \theta \leq 20^0$ and small variations are noticed afterwards. Corresponding to M=0, the variations are similar to GN Type-II for the range $0^0 \leq \theta \leq 40^0$ and then a small jolt is followed by high jump and the values are stationary for $\theta \geq 65^0$.

Amplitude ratio Z_{10}: Fig.22 displays the variations of amplitude ratio Z_{10} with angle of incidence θ. Corresponding to GN-III , the variations are in the form of Dirac Delta function for the range $10^0 \leq \theta \leq 20^0$ and variations in form of descending steps are noticed afterwards. Corresponding to M=0, for the first half range the values are in form of steps and are in form of seismic waves for the rest. For GN Type-II, the variations are similar to M=0 with a difference of magnitude.

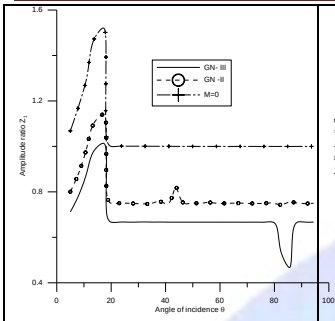

Fig.3 Variations of Amplitude ratio Z_1 with angle of incidence θ.

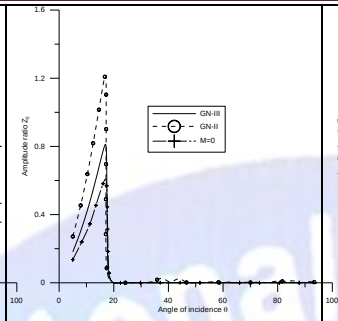

Fig.4 Variations of Amplitude ratioZ_2 with angle of incidence θ.

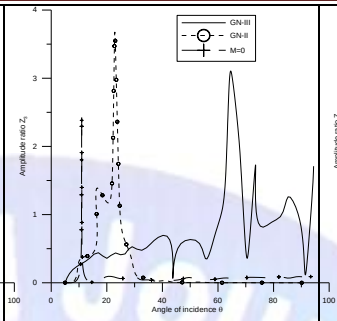

Fig.5 Variations of Amplitude ratio Z_3 with angle of incidence θ.

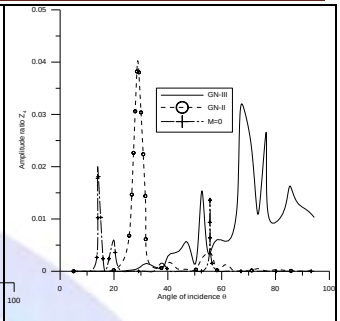

Fig.6 Variations of Amplitude ratio $\boldsymbol{Z_4}$ with angle of incidence $\boldsymbol{\theta}$.

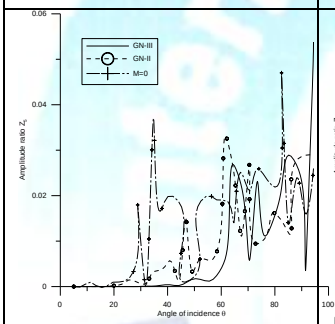

Fig.7 Variations of Amplitude ratio Z_5 with angle of incidence θ.

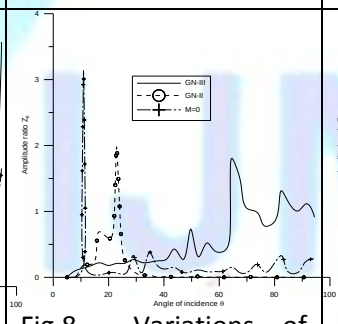

Fig.8 Variations of Amplitude ratio $\boldsymbol{Z_6}$ with angle of incidence θ.

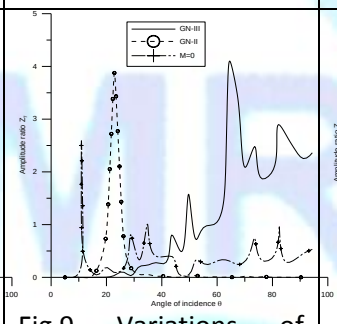

Fig.9 Variations of Amplitude ratio Z_7 with angle of incidence θ.

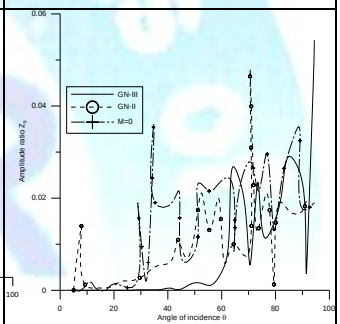

Fig.10 Variations of Amplitude ratio $\boldsymbol{Z_8}$ with angle of incidence θ.

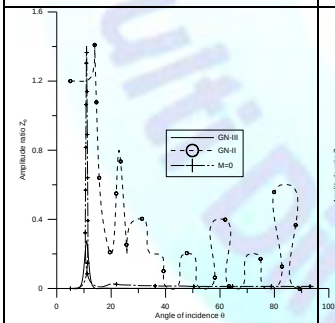

Fig.11 Variations of Amplitude ratio $\boldsymbol{Z_9}$ with angle of incidence θ.

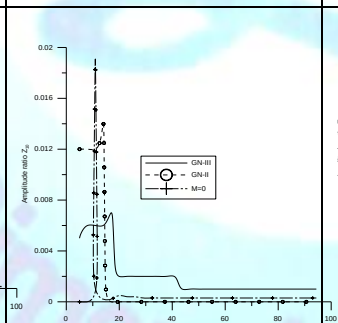

Fig.12 Variations of Amplitude ratio $\boldsymbol{Z_{10}}$ with angle of incidence θ.

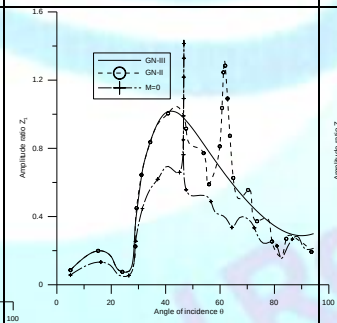

Fig.13 Variations of Amplitude ratio $\boldsymbol{Z_1}$ with angle of incidence θ.

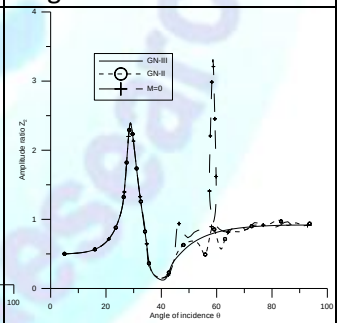

Fig.14 Variations of Amplitude ratioZ_2 angle of incidence θ.

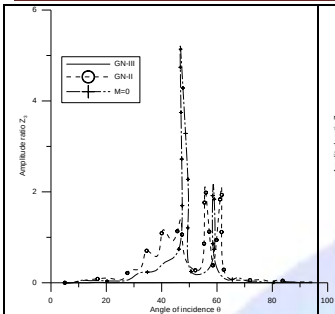

Fig.15 Variations of Amplitude ratio Z_3 with angle of incidence θ.

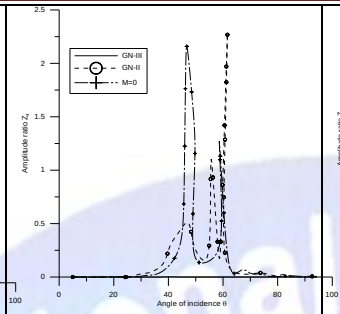

Fig.16 Variations of Amplitude ratio Z_4 with angle of incidence θ.

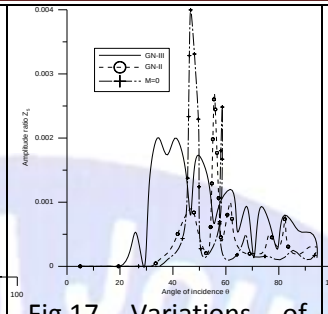

Fig.17 Variations of Amplitude ratio Z_5 with angle of incidence θ.

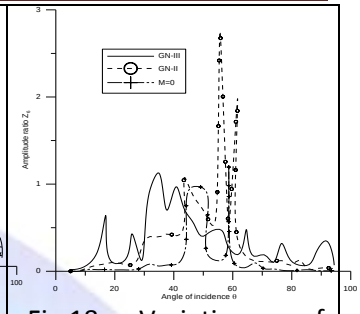

Fig.18 Variations of Amplitude ratio Z_6 with angle of incidence θ.

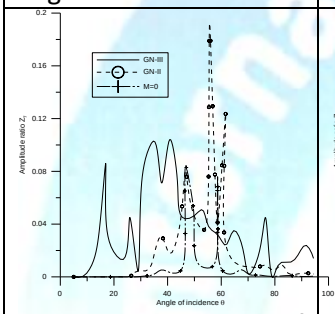

Fig.19 Variations of Amplitude ratio Z_7 with respect to angle of incidence θ

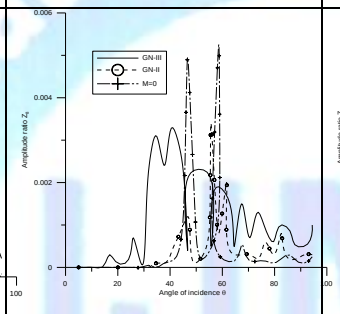

Fig.20 Variations of Amplitude ratio Z_8 with angle of incidence θ.

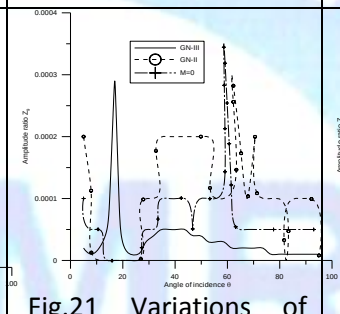

Fig.21 Variations of Amplitude ratio Z_9 with angle of incidence θ.

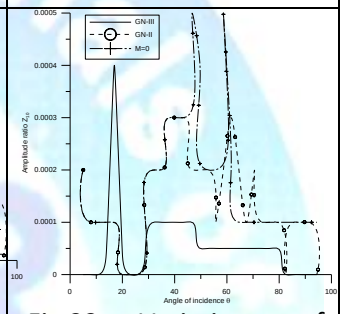

Fig.22 Variations of Amplitude ratio Z_{10} with angle of incidence θ.

8.Conclusion

Important phenomena are noticed in all the graphical representations of amplitude ratios. These phenomenon permit us some concluding remarks

i) Presence of Hall current in the transversely isotropic magnetothermoelastic solid has a significant effect on the values of amplitude ratios of reflected and refracted waves and tends the variations to move in form of seismic waves for both the theories of GN Type- II and III.

ii) Variations corresponding to GN theory of Type-III move away from the boundary surface as θ increases whereas the trends are not same for GN theory of Type-II (when P Wave is incident).

iii) Variations in all the amplitude ratios corresponding to GN theory of Type-II have sharp increase or decrease in the first half range and are very small near boundary surface in the second half range (when P Wave is incident).

iv) Variations are maximum in the middle of the range when SV Wave is incident and are near to the boundary surface initially and finally .

v) These trends obey elastic and thermoelastic properties of a solid under investigation and all the results are in agreement with the thermoelasticity theory with two temperature. The present theoretical results may provide interesting information for experimental scientists/ researchers/ seismologists working on this subject. The used methods in the present article is applicable to a wide range of problems in thermodynamics and thermoelasticity.

9.References

Achenbach, J.D.(1973); Wave propagation in elastic solids.*Elsevier:* North -Holland,Amsterdam.;

Ailawalia,P., and Singla,A.(2016); Disturbance due to internal heat source in a thermoelastic solid using dual phase lag models, *Structural Engineering and Mechanics*,**56**(3),341-354.

Atwa,S.Y; and Jahangir,A(2014); Two temperature effects on plane waves in generalized Thermo-Microstretch Elastic Solid, *International Journal of Thermophysics*,**35,**175-193.

Boley,B.A,and Tolins,I.S,(1962);Transient coupled thermoelastic boundary value problem in the half space, *Journal of Applied Mechanics,* **29**, 637-646.

Chandrasekharaiah, D. S.(1998); Hyperbolic thermoelasticity: A review of recent literature. *Appl. Mech. Rev*., **51** , 705-729.

Chaudhary,S., Kaushik,V.P., and Tomar,S.K(2010);Transmission of plane SH- waves through a monoclinic layer embedded between two different self reinforced elastic solid half-spaces, *Int. J. of Appl. Math and Mech*., **6** (19), 22-43.

Chen,P.J., and Gurtin, M.E(1968); On a theory of heat conduction involving two parameters, *Zeitschrift für angewandte Mathematik und Physik (ZAMP)*, **19**,614-627.

Chen,P.J., Gurtin, M.E., and Williams,W.O(1968); A note on simple heat conduction, *Journal of Applied Mathematics and Physics (ZAMP)*, **19**, 969-70.

Chen,P.J., Gurtin, M.E., and Williams,W.O.(1969); On the thermodynamics of non simple elastic materials with two temperatures, *(ZAMP),* **20**, 107-112.

Das,P; and Kanoria,M.(2014);Study of finite thermal waves in a magnetothermoelastic Rotating medium, *Journal of Thermal Stresses*, **37**(4),405-428 .

Deshpande,V.S., and Fleck,N.A.(2005); One-dimensional response of sandwich plates to underwater shock loading, *Journal of Mechanics and Physics of Solids*,**53**,2347-2383.

Dhaliwal,R.S., and Singh,A.(1980);Dynamic coupled thermoelasticity, *Hindustance Publisher corp,* New Delhi(India), :726.

Elphinstone,M.J.,and Lakhtakia,A.(1994);Plane wave response of an elastic chiral solid slab sandwiched between achiral solid half spaces, *Journal of the Acoustical Society of America* ,**95**,617-627.

Ezzat,M.A., EI-Karamany,A.S.,EI-Bary,A.A.(2016);Modelling of memory dependent derivative in generalized thermoelasticity, ***European Physical Journal Plus*** ,**131**(10), Article:372.

Green, A.E., and Naghdi, P.M.(1991); A re-examination of the basic postulates of thermomechanics.,*Proc. Roy.Soc.London Ser*. **A-432**,171-194.

Green, A.E., and Naghdi, P.M.(1992); On undamped heat waves in an elastic solid, *Journal of Thermal Stresses,* **15**,253-264.

Green, A.E., and Naghdi, P.M.(1993); Thermoelasticity without energy dissipation, *Journal of Elasticity,* **31**, 189-208.

Hilai,I.M., and Othman,I.M.(2016); Propagation of Plane Waves of magneto-thermoelastic medium with voids Influenced by the Gravity and Laser Pulse under G-N Theory, *Multidiscipline Modeling in Materials and Structures* ,12(2),326-344 .

Kaushal.S,Kumar,R.,and Miglani,A.(2011); Wave propagation in temperature rate dependent thermoelasticity with two temperatures ,*Mathematical Sciences*,**5**,125-146.

Kaushal.S,Sharma,N.,and Kumar,R.(2010); Propagation of waves in generalized thermoelastic continua with two temperature, *International Journal of Applied Mechanics and Engineering*,**15**,1111-1127.

Keith,C.M. and Crampin. (1977); Seismic body waves in anisotropic media, reflection and refraction at a plane interface, *Geophys.J.R.astr.Soc*,**49**,181-208.

Khurana,A., and Tomar,S.K.(2009); Longitudinal wave response of a chiral slab interposed between micropolar half-spaces, *International Journal of Solids and Structures*,**46**,15-150.

Kumar,R.(2015); Wave propagation in a microstretch thermoelastic diffusion solid,*VERSITA*,**23**(1),127-169.

Kumar,R., Sharma,N., and Lata,P.(2016);Effects of Hall current in a transversely isotropic magnetothermoelastic with and without energy dissipation due to normal force, *Structural Engineering and Mechanics*,**57**(1),91-103.

Kumar,R; and Kansal,T.(2011);Reflection of plane waves at the free surface of a transversely isotropic thermoelastic diffusive solid half-space, *Int.J.of Appl. Math. and Mech*.,**7**(14),57-78.

Kumar,R; Sharma,N; and Ram,P.(2008);Reflection and transmission of micropolar elastic waves at an imperfect boundary, *Multidiscipline Modeling in Materials and Structures* ,**4** (1), 15-36.

Kumar,R;and Gupta,V.(2013);Plane wave propagation in an anisotropic thermoelastic medium with fractional order derivative and void, *Journal of thermoelasticity,* **1**(1), 21-34.

Kumar,R.,and Mukhopdhyay,S.(2010); Effects of thermal relaxation times on plane wave propagation under two temperature thermoelasticity, *International Journal Of Engineering Sciences*, **48**(2),128-139.

Lee,j;and Lee,S.(2010);General solution of EM wave propagation in anisotropic media, *Journal of the Korean Physical Society*,**57**(1),55-60.

Liu,L.,and Bhattacharya,K.(2009); Wave propagation in a sandwich structure, *International Journal of Solids and Structures*, **46**, 3290-3300.

Marin,M.(2013);Effect of distinct conductive and thermodynamic temperatures on the reflection of plane waves in micropolar half-space,*U.P.B.Sci Bull,SeriesA*, **75**(2),121-132.

Negin,M.(2016); Generalized Rayleigh wave propagation in a covered half-space with liquid upper layer, *Structural Engineering and Mechanics*, **56**(3),491-506.

Othman,M.I.A.(2010);Generalized Electro-Magneto-Thermoelasticity in case of thermal shock wavesfor a finite conducting half-space with two relaxation times, *Mechanics and Mechanical Engineering*,**14**(1),5-30.

Sharma,K.,Bhargava,R.R.(2014);Propagation of thermoelastic plane waves at an imperfect boundary of thermal conducting viscous liquid/generalized thermolastic solid, *Afr.Mat*. ,**25**,81-102.

Sharma,K.,and Marin,M.(2013); Effect of distinct conductive and thermodynamic temperatures on the reflection of plane waves in micropolar elastic half-space,*U.P.B.Sci.Bull Series*,**75**(2),121-132.

Slaughter,W.S.(2002);The linearised theory of elasticity,Birkhausar.

Said,M.S.,and Othman,M.I.A.(2016); Wave propagation in a two temperature fibre-reinforced magneto-thermoelastic medium with three phase lag models, *Structural Engineering and Mechanics,***57**(2),201-220.

Warren, W.E., and Chen,P.J.(1973); Wave propagation in the two temperature theory of thermoelasticity, *Journal of Acta Mechanica,***16**, 21-33.

Youssef, H.M.(2006); Theory of two temperature generalized thermoelasticity, *IMA Journal of Applied Mathematics*,**71**(3),383-390.

Youssef, H.M.(2011); Theory of two - temperature thermoelasticity without energy dissipation*, Journal of Thermal Stresses,* **34**, 138-146.

Appendix A

Where $A = \zeta_4\zeta_5\zeta_6 - cos^2\theta\ \zeta_2\zeta_7 p_1 - \delta_1\zeta_8^2\zeta_1\zeta_4 + \zeta_2\zeta_7\zeta_8 + \zeta_2\zeta_7\zeta_8^2\zeta_1$,

$B = -\zeta_1\zeta_4\zeta_6 - \zeta_1 cos^2\theta\ \zeta_2\zeta_7 p_1 + \omega^2\zeta_6\zeta_5 - \zeta_4\zeta_5\zeta_1 + \zeta_5 cos^2\theta\ \zeta_7 p_1 - \delta_1\zeta_4\zeta_3\zeta_8 + \zeta_2\zeta_7\zeta_8 - \delta_1\omega^2\zeta_1\zeta_8^2 + \zeta_3\zeta_8\zeta_1\zeta_4 - \zeta 1_8^2\zeta_1\zeta_7 - \zeta_2\zeta_8\zeta_3\zeta_7 + \delta_1\zeta_8\zeta_7 + p_1\zeta_7\zeta_6 sin^2\theta - sin^2\theta\ \zeta_2\zeta_7 p_1$

$C = -\zeta_5\zeta_1\omega^2 - \zeta_1\zeta_6\omega^2 + \zeta_1^2\zeta_4 - \zeta_1 cos^2\theta\ \zeta_7 p_1 - \zeta_3\delta_1\omega^2\zeta_8 + \zeta_3^2\zeta_4 + \zeta_8\zeta_3\zeta_1\omega^2 - \zeta_1\ \varepsilon_5'\beta_1^2\omega^2 sin^2\theta$

$D = \omega^2(\zeta_1^2 - \zeta_3^2)$,$\zeta_1 = \left(\frac{\varepsilon_0\mu_0^2 H_0^2}{\rho} + 1\right)\omega^2 + \Omega^2, \zeta_2 = \frac{a_1}{L} sin^2\theta + \frac{a_3}{L} cos^2\theta\ ,\ \zeta_3 = -2i\omega\Omega, \zeta_4 = \zeta_2\omega^2 - sin^2\theta(\varepsilon_1 + i\varepsilon_3) - cos^2\theta\ (\varepsilon_2 + i\varepsilon_4),\quad \zeta_5 = sin^2\theta + \delta_2 cos^2\theta\ ,\quad \zeta_6 = \delta_2 sin^2\theta + \delta_3 cos^2\theta\ ,\ \zeta_7 = \varepsilon_5'\omega^2\beta_1\beta_3\ ,\quad \zeta_8 = -sin\theta cos\theta, p_5 = \frac{\beta_3}{\beta_1}$

Appendix B

$d_j =$
$[k_j^4\{\eta_j(\delta_1 sin^2\theta_j\varepsilon_{13} + \delta_1 cos^2\theta_j\varepsilon_{24} - \delta_1\zeta_j + \varepsilon_5'\beta_1\beta_3\omega^2\zeta_j\} + k_j^2\{-\delta_1\omega^2\eta_j + (M_0 + 2\Omega)i\omega(\varepsilon_{13}sin^2\theta_j + cos^2\theta_j\varepsilon_{24}\} - \omega^2(M_0 + 2\Omega)i\omega\ ]/D\ ,\quad j = 1,2,3$

$l_j =$
$[k_j^3\{-\delta_1\eta_j\varepsilon_5'\beta_1\beta_3\omega^2 icos\theta_j + (\delta_2 isin^3\theta_j + \delta_3 icos^2\theta_j sin\theta_j)\varepsilon_5'\beta_1^2\omega^2\} +$
$ik_j\{(M_0 i\omega + 2i\omega\Omega)(\varepsilon_5'\beta_1\beta_3\omega^2 cos\theta_j) + \left(\frac{M_0}{m}i\omega + \omega^2 + \Omega^2\right)(\varepsilon_5' sin\theta_j\beta_1^2\omega^2)\}]/D\ , j = 1,2,3$

$D = k_j^4(\varepsilon_{13}\delta_2 sin^4\theta_j + \varepsilon_{13}\delta_3\eta_j^2 + \delta_2\varepsilon_{24}\eta_j^2 + \varepsilon_{24}\delta_3 cos^4\theta_j - \delta_2\omega^2 sin^2\theta_j\zeta_j - \omega^2\delta_3 cos^2\theta_j\eta_j - \beta_3^2\varepsilon_5'\omega^2 cos^2\theta_j\eta_j) + k_j^2\left\{(-sin^2\theta_j\delta_2 - \delta_3 cos^2\theta_j)\omega^2 + \left(\frac{M_0}{m}i\omega + \omega^2 + \Omega^2\right)(-\varepsilon_{13}sin^2\theta_j - \varepsilon_{24}cos^2\theta_j + \omega^2\zeta_j) - \beta_3^2\varepsilon_5'\omega^2 cos^2\theta_j\right\} + \left(\frac{M_0}{m}i\omega + \omega^2 + \Omega^2\right)\omega^2\ , j = 1,2,3$

$d_j =$
$[k_j^4\{\eta_j(\delta_1 sin^2\theta_j\varepsilon_{13} + \delta_1 cos^2\theta_j\varepsilon_{24} + \delta_1\zeta_j - \varepsilon_5'\beta_1\beta_3\omega^2\zeta_j\} + k_j^2\{-\delta_1\omega^2\eta_j + (M_0 + 2\Omega)i\omega(\varepsilon_{13}sin^2\theta_j + cos^2\theta_j\varepsilon_{24}\} - \omega^2(M_0 + 2\Omega)i\omega\ ]/D\ ,\quad j = 4,5,6$

$l_j =$
$[k_j^3\{\delta_1\eta_j\varepsilon_5'\beta_1\beta_3\omega^2 icos\theta_j + (\delta_2 isin^3\theta_j + \delta_3 icos^2\theta_j sin\theta_j)\varepsilon_5'\beta_1^2\omega^2\} +$
$ik_j\{(M_0 i\omega + 2i\omega\Omega)(\varepsilon_5'\beta_1\beta_3\omega^2 cos\theta_j) + \left(\frac{M_0}{m}i\omega + \omega^2 + \Omega^2\right)(\varepsilon_5' sin\theta_j\beta_1^2\omega^2)\}]/D\ j = 4,5,6$

$\eta_j = sin\theta_j cos\theta_j\ , \varepsilon_{13} = \varepsilon_1 - i\varepsilon_3\omega, \varepsilon_{24} = \varepsilon_2 - i\varepsilon_4\omega, \zeta_j = \frac{a_1}{L} sin^2\theta_j + \frac{a_3}{L} cos^2\theta_j\ , M_0 = \frac{M}{1+m^2}\ \mu_0 H_0 m$

Appendix C

$a_{11} = i\sin\theta\ ,\ a_{12} = i/\beta'^{(1)}\sqrt{\omega^2 - \beta'^{(1)^2} sin^2\theta}, a_{13} = -1, a_{14} = -1, a_{15} = -1, a_{16} = -1, a_{17} = -1, a_{18} = -1, a_{19} = 0, a_{1,10} = 0, a_{21} = -i/\alpha'^{(1)}\sqrt{\omega^2 - \alpha'^{(1)^2}(sin^2\theta)},\ a_{22} = isin\theta, a_{23} = -d_1, a_{24} = -d_2, a_{25} = -d_3, a_{26} = -d_4, a_{27} = -d_5, a_{28} = -d_6, a_{29} = 0\ , a_{2,10} = 0\ , a_{31} = (\omega^2 - \alpha'^{(1)^2})(sin\theta)^2 - \frac{\alpha'^{(1)^2}\gamma'^{(1)^2}}{\omega^2}(sin\theta)^2, a_{32} = \frac{(\alpha'^{(1)^2} - \gamma'^{(1)^2})}{\beta'^{(1)}} sin\theta\sqrt{\omega^2 - \beta'^{(1)^2} sin^2\theta}$

$a_{3j} = -\Delta_j, j =$3,4,5 where $\Delta_j = \frac{c_{11}}{\rho c_1^2} i\ sin\theta + \frac{c_{13}}{\rho c_1^2} i\frac{d_j}{v_j}\sqrt{\omega^2 - v_j{}^2(sin\theta)^2} - \frac{\beta_3}{\beta_1} l_j\left(1 - \frac{v_j{}^2}{\omega^2} sin^2\theta\frac{a_1}{L}\right) - \frac{\beta_3}{\beta_1}\frac{a_3 l_j\omega}{L v_j{}^2}\sqrt{\omega^2 - v_j{}^2(sin\theta)^2}$, $a_{3j} = -\Delta_j', j =$6,7,8, where $\Delta_j' = \frac{c_{11}}{\rho c_1^2} i\ sin\theta - \frac{c_{13}}{\rho c_1^2} i\frac{d_j}{v_j}\sqrt{\omega^2 - v_j{}^2(sin\theta)^2} -$

$\frac{\beta_3}{\beta_1} l_j \left(1 - \frac{{v_j}^2}{\omega^2} sin^2\theta \frac{a_1}{L}\right) - \frac{\beta_3}{\beta_1} \frac{a_3 l_j \omega}{L {v_j}^2} \sqrt{\omega^2 - {v_j}^2 (sin\theta)^2}$, $a_{39} = 0$,

$a_{3,10} = 0, a_{41} = \frac{{\beta'^{(1)}}^2}{\alpha'^{(1)}} \sqrt{\omega^2 - {\alpha'^{(1)}}^2 (sin\theta)^2}$, $a_{42} = \omega^2 - {v_1}^2 (sin\theta)^2$, $a_{4j} = -\eta_j, j = 3,4,5,6,7,8$

where $\eta_j = \frac{c_{44}}{\rho c_1^2} \left(\frac{-i\sqrt{\omega^2 - {v_j}^2 (sin\theta)^2}}{v_j} + \frac{d_j i\omega}{v_j} sin\theta \right), j = 3,4,5$ and $\eta_j = \frac{c_{44}}{\rho c_1^2 s} \left(\frac{i\sqrt{\omega^2 - {v_j}^2 (sin\theta)^2}}{v_j} + \right.$

$\left. \frac{d_j i\omega}{v_j} sin\theta \right), j = 6,7,8, a_{49} = 0, a_{4,10} = 0, a_{5j} = 0, j = 1,2,9,10.\ a_{5j} = \frac{l_j}{v_j} \sqrt{\omega^2 - {v_j}^2 (sin\theta)^2}$,

$j = 3,4,5, a_{5j} = -\frac{l_j}{v_j} \sqrt{\omega^2 - {v_j}^2 (sin\theta)^2}, j = 6,7,8., a_{6j} = 0, j = 1,2.\ a_{69} = isin\theta, a_{6,10} = -i/$

$\beta'^{(2)} (\sqrt{\omega^2 - {\beta'^{(2)}}^2 (sin^2\theta)}, a_{6j} = -1, j = 3,4,5,6,7,8., a_{7j} = 0, j = 1,2, a_{7j} = -d_j, j = 3,4,5,6,7,8.,$

$a_{79} = i\omega / {\alpha'^{(2)}}^2 \sqrt{\omega^2 - {\alpha'^{(2)}}^2 (sin\theta)^2}$, $a_{7,10} = isin\theta, a_{8j} = 0, j = 1,2, a_{8j} = -\Delta_j, j =$3,4,5 where

$\Delta_j = \frac{c_{11}}{\rho c_1^2} i\ sin\theta + \frac{c_{13}}{\rho c_1^2} i \frac{d_j}{v_j} \sqrt{\omega^2 - {v_j}^2 (sin\theta)^2} - \frac{\beta_3}{\beta_1} l_j \left(1 - \frac{{v_j}^2}{\omega^2} sin^2\theta \frac{a_1}{L}\right) - \frac{\beta_3}{\beta_1} \frac{a_3 l_j \omega}{L {v_j}^2} \sqrt{\omega^2 - {v_j}^2 (sin\theta)^2}$,

$a_{8j} = -\Delta'_j, j =$6,7,8, where $\Delta'_j = \frac{c_{11}}{\rho c_1^2} i\ sin\theta - \frac{c_{13}}{\rho c_1^2} i \frac{d_j}{v_j} \sqrt{\omega^2 - {v_j}^2 (sin\theta)^2} - \frac{\beta_3}{\beta_1} l_j \left(1 - \frac{{v_j}^2}{\omega^2} sin^2\theta \frac{a_1}{L}\right) -$

$\frac{\beta_3}{\beta_1} \frac{a_3 l_j \omega}{L {v_j}^2} \sqrt{\omega^2 - {v_j}^2 (sin\theta)^2}$, $a_{89} = -{\gamma'^{(2)}}^2 sin^2\theta - (\omega^2 - {\alpha'^{(2)}}^2 sin^2\theta)$,

$a_{8,10} = \frac{sin\theta}{\beta'^{(2)}} \sqrt{\omega^2 - {\beta'^{(2)}}^2 sin^2\theta}\ (\gamma'^{(2)} + \frac{{\alpha'^{(2)}}^2}{\omega^2})$, $a_{9j} = 0$, $j = 1,2$, $a_{4j} = -\eta_j, j = 3,4,5,6,7,8$ where

$\eta_j = \frac{c_{44}}{\rho c_1^2} \left(\frac{-i\sqrt{\omega^2 - {v_j}^2 (sin\theta)^2}}{v_j} + \frac{d_j i\omega}{v_j} sin\theta \right), j = 3,4,5$ and $\eta_j = \frac{c_{44}}{\rho c_1^2} \left(\frac{i\sqrt{\omega^2 - {v_j}^2 (sin\theta)^2}}{v_j} + \frac{d_j i\omega}{v_j} sin\theta \right), j =$

$6,7,8, a_{99} = \frac{sin\theta}{\alpha'^{(2)}} \sqrt{\omega^2 - {\alpha'^{(2)}}^2 sin^2\theta}$, , $a_{9,10} = sin^2\theta + \frac{\omega^2 - {\beta'^{(2)}}^2 (sin^2\theta)}{\omega^2}$, $a_{10,j} = 0, j = 1,2,9,10.$

$a_{10,j} = \frac{l_j}{v_j} \sqrt{\omega^2 - {v_j}^2 (sin\theta)^2}, j = 3,4,5, a_{10,j} = -\frac{l_j}{v_j} \sqrt{\omega^2 - {v_j}^2 (sin\theta)^2}, j = 6,7,8., d_1 = -a_{11},$

$d_2 = a_{21}, d_3 = -a_{31}, d_4 = a_{41}, d_j = 0, j = 5,6,7,8,9,10$

For incident SV wave

$d_1 = -a_{12}, d_2 = -a_{22}, d_3 = -a_{32}, d_4 = -a_{42}, d_j = 0, j = 5,6,7,8,9,10$